Recovery of Missing Samples in Fetal Heart Rate Recordings with Gaussian Processes

Guanchao Feng[*], *J. Gerald Quirk*[†], and *Petar M. Djurić*[*]
[*] Department of Electrical and Computer Engineering
[†] Department of Obstetrics/Gynecology, Stony Brook University Hospital
Stony Brook University
Stony Brook, NY 11794, USA
Email: [*]{guanchao.feng, petar.djuric}@stonybrook.edu, [†]J.Gerald.Quirk@stonybrookmedicine.edu

***Abstract*—Missing samples are very common in fetal heart rate (FHR) recordings due to various reasons including fetal or maternal movements and misplaced electrodes. They introduce distortions and cause difficulties in their analysis. In this paper, we propose a Gaussian process–based method that can utilize other intrapartum signals (e.g., uterine activity and maternal heart rate) to recover the missing samples in FHR recordings. The proposed approach was tested on a short real FHR recording segment and its performance was compared with that of cubic spline interpolation which is widely used in pre-processing of FHR recordings. Our results show that the proposed approach, with utilization of UA signals, achieves 2.35 dB to 14.85 dB better recovery performance. Furthermore, even when the percentage of missing samples is more than 50%, the mean square error of this approach is still below one beat per minute.**

I. Introduction

The most common approach of monitoring fetal well-being in labor is by Cardiotocography (CTG), which measures FHR and uterine activity (UA) signals. Both signals are visually inspected by clinicians. Clinical guidelines regarding FHR evaluation are available from both the National Institute of Child Health and Human Development (NICHD) and the International Federation of Gynecology and Obstetrics (FIGO) [1], [2]. However, it is well known that the interpretation of FHR signals is prone to high intra- and inter-observer variability due to subjectivity in visual inspections. Moreover, current guidelines for FHR evaluation have been criticized for simplistic interpretation and held responsible for defensive practices as well as unnecessary operative interventions [3].

To combat these problems, various automated FHR analysis and evaluation approaches have been proposed since 1980s. They are inherently objective and have the ability to extract features and discovery patterns that cannot be seen by naked human eyes. For example, in [4], the authors developed methods that are based on generative models (GMs) and Bayesian theory for FHR classification, where two categories, healthy and unhealthy, are defined using umbilical cord pH values which is the gold-standard for diagnosis. The results have shown that GMs and the Bayesian paradigm can significantly improve automatic FHR classification. Recently, the use of hierarchical Dirichlet process (HDP) mixture models in FHR analysis has been proposed [5], and the results of FHR classification are very promising. There are also methods with good results that have adopted artificial neural networks [6], [7]. Although the literature on this topic has been mainly concentrated on FHR, it is not the only available source of information about fetal well-being. Other intrapartum signals, the UA and MHR, also contain information about fetal status.

In sampling of FHR, various reasons, such as fetal or maternal movements and misplaced electrodes, can cause missing samples and distortions. For external ultrasound measurements, the percentage of missing samples varies from 0-40%, and for internal direct fetal ECG measurement such percentage varies from 0-10%. We should notice that there are still no guidelines on what percentage of missing samples will disqualify an FHR recording from visual inspection or from automatic analysis, although an empirical value given by clinicians, for visual inspection, is 50%. One can argue that clinicians can tolerate such high percentages of missing samples in FHR because i) their inspections, unlike automated systems, are mainly focused on morphological features and ii) the human visual perception is very robust to loss of samples.

In the suppression of distortions in automated FHR analysis, the first step is usually pre-processing, which aims at improving the quality of FHR recordings. This often involves artifacts removal (a popular algorithm is described in [8]), interpolation, and gap treatments. More specifically, in practice, small segments of missing samples are interpolated using linear or cubic spline interpolation, while bigger segments, for example, segments of duration of 15 seconds or more, are often entirely removed. [9].

Features that describe different characteristics of FHR and that carry information about fetal well-being are then extracted from pre-processed FHR recordings. To that end, for instance, one employs short term variability (STV), long term variability (LTV) and entropy. The pre-processing step is essential in FHR analysis because the quality of the pre-processing is directly related to the values of the features, and therefore, the performance of the analysis [10]. For instance, in [11], the authors investigated the stability of several STV and LTV features when 0-50% missing samples were randomly selected in a 5-minute FHR segment within the first stage of labor. These missing samples were then linearly interpolated before computing the features. The results indicated that the values of many features have changed considerably. The conclusion is

ISBN 978-0-9928626-7-1

that missing samples, if not properly recovered or addressed, may cause serious problems in the automated analysis.

The recovery of missing FHR samples is a topic that has been largely overlooked in the literature on FHR analysis. Only recently, an adaptive method that includes two steps for this purpose was introduced [12]. During the first step, missing samples are estimated using an empirical dictionary, and in the second step, the dictionary is re-constructed using the updated data from the first step. These two steps are applied iteratively until convergence. This adaptive method has achieved 2 to 4.5 dB better reconstruction ability compared to the cubic spline interpolation. However, in many other communities such as image processing, machine learning and geo-statistics, recovery of missing data has been extensively explored. In geo-statistics, which is widely used in mining of mineral resources, a common task is to estimate grades and other parameters from a relatively small set of borehole or other samples. A powerful and effective approach for this task is kriging. This method has been developed and applied to many other fields including machine learning, where it is known as Gaussian process (GP) prediction [13].

In this paper, we propose an effective GP–based approach, that not only uses information in observed FHR samples but also relies on UA signals for the recovery of missing FHR samples. Although the MHR can also be easily incorporated, we have not used it because the database for our experiments (described in [14]) does not have it. If a missing FHR sample is located far away (in time) from the observed FHR samples in a recording, such observed samples contain very limited information about that missing sample. However, its nearby UA and MHR samples may contain valuable information about its true value. For each missing FHR sample, a full predictive Gaussian distribution of the missing sample is provided. This offers more insight than a simple point estimate and an error bar.

The paper is organized as follows. In the next section, we provide a brief background on data acquisition and GPs. In Section 3, we present our GP–based method in details. In the following section, we first describe the open access intrapartum CTG database we used for our experiments, then we show how we implement our GP-based method on a segment of real FHR recording and finally, we compare its performance with that of the cubic spline interpolation. Then we conclude the paper with some final remarks in Section 5.

II. Background

A. Data Acquisition

Electronic Fetal Monitoring (EFM) is predominantly utilized for assessing fetal status immediately preceding or during labor through the use of CTG, which monitors FHR and UA simultaneously. Changes in FHR is recorded via Doppler ultrasound (external) or direct fetal ECG measurement (internal) with a fetal scalp electrode, and UA is usually monitored externally with a tocodynamometer. External CTG is more popular since it is non-invasive and is very suitable for continuous or intermittent monitoring. However, it usually provides less accurate and/or missing measurements [15]. An example of this is given by Fig. 1, where many missing samples are presented in FHR.

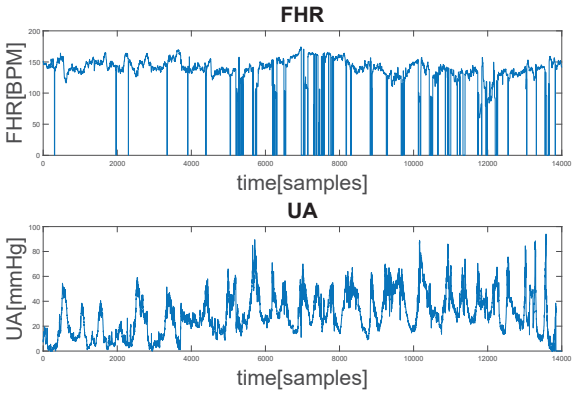

Fig. 1. A segment of un-preprocessed (raw) FHR and the corresponding UA.

B. Gaussian Processes

Gaussian processes have been successful in both supervised and unsupervised machine learning tasks. Here we focus on the regression framework of GPs since recovery of missing FHR samples is indeed a regression problem. A GP, by definition, is a collection of random variables with a joint Gaussian distribution. A GP extends a multivariate Gaussian distribution to infinite dimensionality, and therefore, can be seen as the distribution of a real-valued function $f(\mathbf{x})$, where the location index $\mathbf{x}$ is generally a vector. For every fixed $\mathbf{x}$, $f(\mathbf{x})$ is a real-valued random vector. The infinite dimensionality is, in fact, easy to work with, because of the consistency (also known as marginalization property) and computational tractability offered by GPs.

A Gaussian distribution can be fully characterized by its mean and variance. Similarly, a Gaussian process is completely specified by its mean function $m(\mathbf{x})$ and covariance function $k_f(\mathbf{x}_i, \mathbf{x}_i)$, which are defined as

$$m(\mathbf{x}) = E[f(\mathbf{x})], \tag{1}$$

and

$$k_f(\mathbf{x}_i, \mathbf{x}_j) = E[(f(\mathbf{x}_i) - m(\mathbf{x}_i))(f(\mathbf{x}_j) - m(\mathbf{x}_j))]. \tag{2}$$

The prior distribution of $f(\mathbf{x})$ is constructed through k_f, in which the covariance of two random variables, $f(\mathbf{x}_i)$ and $f(\mathbf{x}_j)$, depends on their locations, $\mathbf{x}_i$ and $\mathbf{x}_j$. Usually the mean of a GP is assumed to be zero for simplicity, that is, $m(\mathbf{x}) = 0$ for every $\mathbf{x}$. The design of appropriate covariance functions is the key to a successful use of GPs because they carry our beliefs about the characteristics of $f(\mathbf{x})$.

One of the widely-used covariance functions is the squared exponential covariance function, which for the 1-D case has the following form:

$$k_{SE}(x_i, x_j) = \exp(-\frac{1}{l}(x_i - x_j)^2), \tag{3}$$

ISBN 978-0-9928626-7-1 © EURASIP 2017

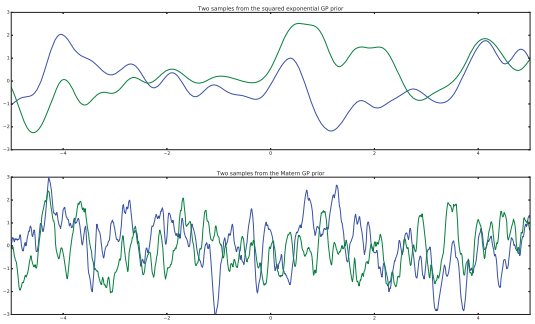

Fig. 2. Two function samples from GP priors constructed by squared exponential (upper) and Matern (bottom, $\nu = 3/2$) covariance functions, respectively, with the same length-scale of $l = 0.1$.

where the length-scale $l > 0$ is its hyper-parameter. Because squared exponential covariance functions are infinitely differentiable, the resulting GPs have mean square derivatives of all orders and therefore are very smooth, as illustrated in Fig. 2.

Another class of popular covariance functions in the machine learning community is known as Matérn class of functions. One parameter that defines them is known as ν, and it can be shown that, when ν is half integer, the Matérn covariance functions become simply a product of an exponential and a polynomial. The 1-D form corresponding to $\nu = 3/2$ and $\nu = 5/2$ are as follows:

$$k_{\nu=3/2}(r) = \left(1 + \sqrt{3}r/l\right) \exp\left(-\sqrt{3}r/l\right), \tag{4}$$

and

$$k_{\nu=5/2}(r) = \left(1 + \sqrt{5}r/l + 5r^2/(3l^2)\right) \exp\left(-\sqrt{5}r/l\right), \tag{5}$$

where r is the distance between x_i and x_j. To illustrate the different characteristics of the resulting functions, in Fig. 2, we present two functions generated by a GP prior with a squared exponential covariance function and a GP with a Matérn ($\nu = 3/2$) covariance function, both with the same length-scale $l = 0.1$. More information on GPs can be found in [13].

III. Model Description

We assume that the observed value of the ith sample y_i in an FHR segment is a function of i and its synchronized UA sample, u_i, with additive Gaussian white noise, i.e.,

$$y_i = y(\mathbf{x}_i) = f(\mathbf{x}_i) + \epsilon, \tag{6}$$

where $\mathbf{x}_i = [i, u_i]'$ is a 2-D vector, $f(\mathbf{x}_i)$ is a latent variable, and $\epsilon \sim \mathcal{N}(0, \sigma^2)$ is Gaussian white noise. We observe a segment of an FHR recording of length L with n observed samples, and we assume that it is synchronized with a UA segment which does not have missing samples and artifacts, and we want to use it to perform training. Our goal is that after training we are able to estimate the missing FHR samples. For simplicity, we also use a zero mean function, $m(\mathbf{x}) = 0$.

As shown in Fig. 1, FHR signals can be seen as a superposition of a slow varying component and a rapid varying component. Therefore, we construct our covariance function (for $f(\mathbf{x})$) as a summation of a squared exponential covariance function, a Matérn covariance function (when $\nu = 3/2$) and a linear covariance function (for capturing linearity). It is defined as follows:

$$\begin{aligned} k_f(\mathbf{x}_i, \mathbf{x}_j) = {\alpha_1}^2 &\left[1 + \sqrt{3}[(\mathbf{x}_i - \mathbf{x}_j)'\Lambda_1(\mathbf{x}_i - \mathbf{x}_j)]^{\frac{1}{2}}\right] \\ &\times \exp\left[-\sqrt{3}[(\mathbf{x}_i - \mathbf{x}_j)'\Lambda_1(\mathbf{x}_i - \mathbf{x}_j)]^{\frac{1}{2}}\right] \\ &+ {\alpha_2}^2 \exp\left[-\frac{1}{2}[(\mathbf{x}_i - \mathbf{x}_j)'\Lambda_2(\mathbf{x}_i - \mathbf{x}_j)]^{\frac{1}{2}}\right] \\ &+ \left[(\mathbf{x}_i)'\Lambda_3(\mathbf{x}_j)\right], \end{aligned} \tag{7}$$

where $\Lambda_1 = \begin{pmatrix} \beta_1 & 0 \\ 0 & \beta_2 \end{pmatrix}$, $\Lambda_2 = \begin{pmatrix} \beta_3 & 0 \\ 0 & \beta_4 \end{pmatrix}$ and $\Lambda_3 = \begin{pmatrix} \beta_5 & 0 \\ 0 & \beta_6 \end{pmatrix}$.

Since we assume the existence of additive white Gaussian noise with variance of σ^2 in the observations, the covariance function of $y(\mathbf{x})$ becomes

$$k_y(\mathbf{x}_i, \mathbf{x}_j) = k_f(\mathbf{x}_i, \mathbf{x}_j) + \sigma^2\delta_{ij}, \tag{8}$$

or its equivalent matrix form is given by

$$\mathbf{K} = cov(\mathbf{y}) = \mathbf{K}_f + \sigma^2\mathbf{I}, \tag{9}$$

where $\mathbf{y} = [y_1, y_2, \cdots, y_n]^\top$, $\mathbf{K}$ and $\mathbf{K}_f$ are covariance matrices of size n, and δ_{ij} is the Kronecker delta function. The entries of $\mathbf{K}_f$ are specified by (7), and the entries of $\mathbf{K}$ by (8).

The hyper-parameter $\boldsymbol{\theta} = [\alpha_1, \alpha_2, \beta_1, \cdots, \beta_6, \sigma]'$ can be learned from the training data using maximum marginal likelihood. It can be shown that the partial derivatives of the marginal likelihood w.r.t. θ_j have the following form:

$$\frac{\partial \log p(\mathbf{y}|\mathbf{X}, \boldsymbol{\theta})}{\partial \theta_j} = \frac{\mathbf{y}^T\mathbf{K}^{-1}\frac{\partial \mathbf{K}}{\partial \theta_j}\mathbf{K}^{-1}\mathbf{y} - tr\left(\mathbf{K}^{-1}\frac{\partial \mathbf{K}}{\partial \theta_j}\right)}{2}, \tag{10}$$

where $\mathbf{X} = [\mathbf{x}_1, \mathbf{x}_2, \cdots, \mathbf{x}_n]$. The vector $\boldsymbol{\theta}$ can be tuned by adopting a gradient based optimizer.

For a missing FHR sample at location $\mathbf{x}_*$, the mean and covariance of $f(\mathbf{x}_*)$ are given by:

$$E(f(\mathbf{x}_*)) = [\mathbf{k}_f(\mathbf{x}_*, \mathbf{X})]^T\mathbf{K}^{-1}\mathbf{y}, \tag{11}$$

and

$$\sigma^2_{f(\mathbf{x}_*)} = k_f(\mathbf{x}_*, \mathbf{x}_*) - [\mathbf{k}_f(\mathbf{x}_*, \mathbf{X})]^T\mathbf{K}^{-1}\mathbf{k}_f(\mathbf{x}_*, \mathbf{X}), \tag{12}$$

where $\mathbf{k}_f(\mathbf{x}_*, \mathbf{X}) = [k_f(\mathbf{x}_*, \mathbf{x_1}), k_f(\mathbf{x}_*, \mathbf{x_2}), \cdots, k_f(\mathbf{x}_*, \mathbf{x_n})]^\top$ is a column vector of length n whose entries are defined by (7). We use $E(f(\mathbf{x}_*))$ as the recovered FHR value at $\mathbf{x}_*$ since the mode of a Gaussian distribution is also its expectation.

The length of the FHR segment, L, needs to be selected carefully for efficient implementation. This length should not be very long, since FHR samples that precede long time before or come much later after an unobserved sample do not contain

ISBN 978-0-9928626-7-1 © EURASIP 2017

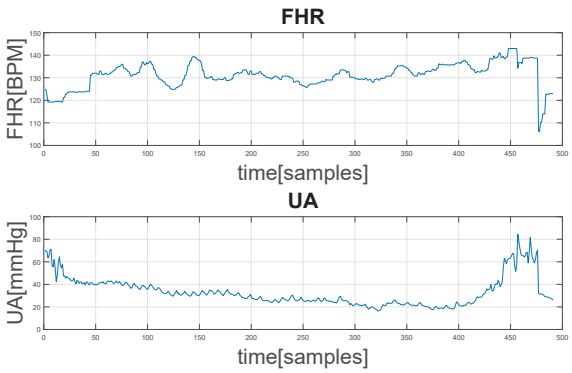

Fig. 3. FHR segment (upper) and its correponding UA segment (bottom) that are adopted for our experiments.

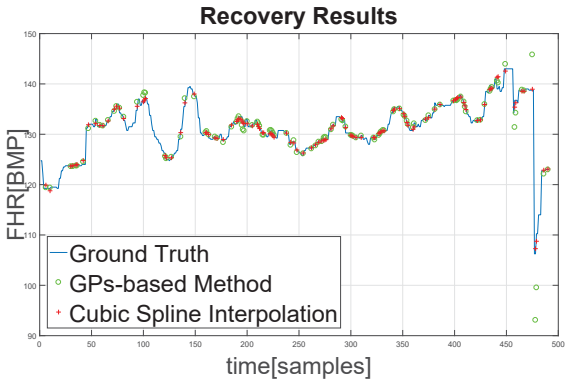

Fig. 4. Recovery results for the 120 missing samples of GPs-based method and cubic spline interpolation.

much information about the sample. On the other hand, if the segment is too short, we may not have enough information to recover the missing samples. One reasonable way to choose L is to refer to the corresponding UA signal. The patterns in the UA signal have quasi-periodic characteristics, and a major contraction approximately takes about 1.5 to 2.0 minutes. Typically, the FHR and UA are sampled with a frequency of 4 Hz, and therefore, such segments have 360 to 480 samples. Long FHR segments can also be accommodated. We can buffer them into overlapped short frames and then implement recovery within the frames. Then the final recovered value of a sample is obtained from all the estimated values of the sample.

IV. Experiments and Results

A. Open Access Intrapartum CTG Database

In our experiments, we used an open access database which contains 552 intrapartum CTG recordings (506 vaginal deliveries and 46 cesarean sections) and corresponding clinical data. The data were acquired between April 2010 and August 2012 at the obstetrics ward of the University Hospital in Brno, Czech Republic. Each CTG recording contains FHR and UA, both sampled at 4 Hz. Most of the recordingswere externally obtained using ultrasound. If a signal was recorded via an internal scalp electrode, it also contained T/QRS ratio and information about the biphasic T-wave. There are 552 recordings, and they were carefully selected from 9,164 recordings using many clinical and technical criteria, for instance, a maximum of 60 minutes for the first stage labor, a maximum of 30 minutes for the second stage labor. No more than 50% of a signal was allowed to be missing in the first stage labor. A detailed description of the database can be found in [14].

B. Test on Real Data

In this example, we selected a CTG segment that contained 491 consecutive samples without missing samples and obvious artifacts, as shown in Fig. 3. Then, 120 samples of the FHR signal were randomly selected and considered missing (their values were set to zero), and we tried to recovery them. The results from the GP–based method and the cubic spline interpolation are shown in Fig. 4. Clearly, the GP–based method provided better results. Its recovery results are much closer to the ground truth, especially at time instants where the ground truth undergoes rapid changes.

C. Benchmark Results

The metrics for measuring the recovery performance was the mean squared error (MSE) in logarithmic scale and the signal-to-noise ratio (SNR), which are defined by

$$\text{Log of MSE} = \log_e(\|\mathbf{s} - \hat{\mathbf{s}}\|^2 / N), \tag{13}$$

and

$$\text{SNR} = 10\log_{10}(\|\mathbf{s}\|^2 / \|\mathbf{s} - \hat{\mathbf{s}}\|^2), \tag{14}$$

where N is the number of missing samples, $\mathbf{s}$ is ground truth and $\hat{\mathbf{s}}$ is reconstructed signal.

From the same CTG segment in the previous example, we selected a percentage of FHR samples to be considered missing (their corresponding UA values were observed). We drew the samples uniformly and then tried to estimate them. The percentage of missing samples was increased from 1% to 85% with a step size of 1%. In order to get a reliable benchmark of performance, for each specific percentage, the experiment was repeated 90 times, and both metrics were averaged over the 90 experiments. The benchmark results are shown in Fig. 5, where the performance of the cubic spline interpolation was included for reference.

The improved performance of our method was confirmed with both metrics. Our GP-based method achieved 2.35 dB to 14.85 dB better recovery performance compared to the cubic spline interpolation. Even when the percentage of missing samples was more than 50%, the MSE of our approach was still below one beat per minute.

D. Benefits of utilizing UA

To demonstrate the contribution of the UA signal in the recovery, we repeated the first example, but excluded u_i from the input vector $\mathbf{x}_i$, and applied the same covariance function (we reduced it from 2-D to 1-D). Then for both cases, with and without the UA signal, and for every time

ISBN 978-0-9928626-7-1 © EURASIP 2017

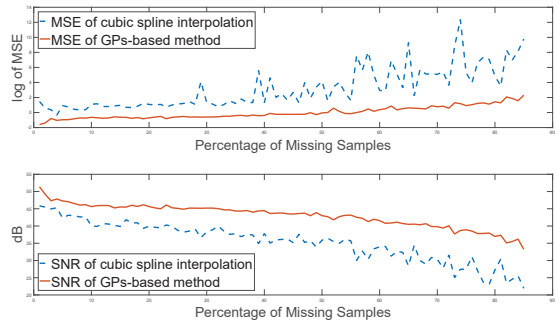

Fig. 5. The MSE (upper plot, in log scale) and SNR (bottom plot) of each method when different percentages of missing samples are presented, averaged over 90 experiments.

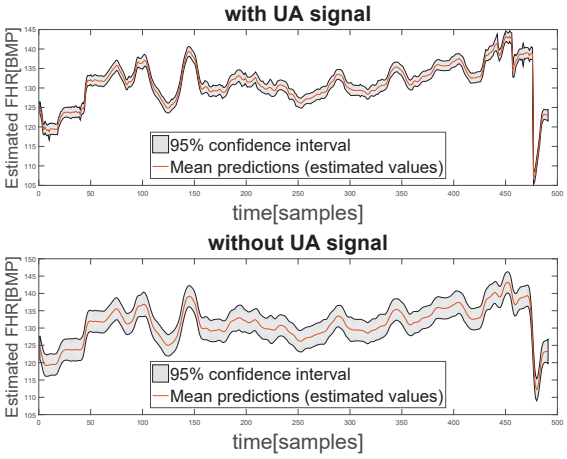

Fig. 6. Estimates of missing values with confidence intervals when UA is utilized (upper plot) and when UA is not utilized (bottom plot).

instant (from 1 to 491), we plotted the estimated values of the latent variables $f(\mathbf{x})$ and $f(x)$, along with the 95% confidence intervals as shown in Fig. 6. The shaded area (which corresponds to the 95% confidence interval) with the use of UA is much narrower. This indicates that with the UA signal the model can better explain the training data and predict much more confidently. The comparison of the performance is given in Table I. From the results, we see that without the UA signal the performance has deteriorated noticeably. We also note that the method continued to do better than the cubic spline interpolation.

TABLE I
COMPARISONS OF PERFORMANCE

Recovery method	MSE[BPM]	SNR[dB]
GP-based method, with UA	0.3311	47.1805
GP-based method, without UA	1.3572	41.0835
Cubic spline interpolation	3.5031	36.9352

V. Conclusion and Future Work

In this paper, we proposed a GP–based method that employs other intrapartum signals for recovery of FHR samples. According to test results on real CTG data, this method offers more accurate and reliable results than the cubic spline interpolation which is widely applied in pre-processing of FHR signals. Even with high percentage of missing samples, the recovery results are very good. Our work also provided evidence that UA signals contain information about fetal well-being. It is reasonable to believe that incorporating MHR signals will further improve the recovery performance of our approach. Our future work includes addressing settings where the UA signal itself has missing values.

References

[1] D. Ayres-de Campos, C. Y. Spong, E. Chandraharan, and F. I. F. M. E. C. Panel, "FIGO consensus guidelines on intrapartum fetal monitoring: Cardiotocography," *International Journal of Gynecology & Obstetrics*, vol. 131, no. 1, pp. 13–24, 2015. [Online]. Available: http://dx.doi.org/10.1016/j.ijgo.2015.06.020

[2] G. A. Macones, G. D. Hankins, C. Y. Spong, J. Hauth, and T. Moore, "The 2008 National Institute of Child Health and Human Development workshop report on electronic fetal monitoring: Update on definitions, interpretation, and research guidelines," *Journal of Obstetric, Gynecologic, & Neonatal Nursing*, vol. 37, no. 5, pp. 510–515, 2008.

[3] A. Ugwumadu, "Are we (mis)guided by current guidelines on intrapartum fetal heart rate monitoring? Case for a more physiological approach to interpretation," *BJOG: An International Journal of Obstetrics & Gynaecology*, vol. 121, no. 9, pp. 1063–1070, 2014. [Online]. Available: http://dx.doi.org/10.1111/1471-0528.12900

[4] S. Dash, J. G. Quirk, and P. M. Djurić, "Fetal heart rate classification using generative models," *IEEE Transactions on Biomedical Engineering*, vol. 61, no. 11, pp. 2796–2805, Nov 2014.

[5] K. Yu, J. G. Quirk, and P. M. Djurić, "Fetal heart rate analysis by hierarchical dirichlet process mixture models," in *2016 IEEE International Conference on Acoustics, Speech and Signal Processing (ICASSP)*, March 2016, pp. 709–713.

[6] A. Georgieva, S. J. Payne, M. Moulden, and C. W. Redman, "Artificial neural networks applied to fetal monitoring in labour," *Neural Computing and Applications*, vol. 22, no. 1, pp. 85–93, 2013.

[7] H. Ocak and H. M. Ertunc, "Prediction of fetal state from the cardiotocogram recordings using adaptive neuro-fuzzy inference systems," *Neural Computing and Applications*, vol. 23, no. 6, pp. 1583–1589, 2013.

[8] J. Bernardes, C. Moura, M. de Sa, P. Joaquim, and L. Pereira Leite, "The Porto system for automated cardiotocographic signal analysis," *Journal of Perinatal Medicine-Official Journal of the WAPM*, vol. 19, no. 1-2, pp. 61–65, 1991.

[9] J. C. Sprott and J. C. Sprott, *Chaos and time-series analysis*. Citeseer, 2003, vol. 69.

[10] J. Spilka, "Complex approach to fetal heart rate analysis: A hierarchical classification model," *Czech Technical University, Faculty of Electrical Engineering, Prague*, pp. 35–47, 2013.

[11] J. Spilka, V. Chudáček, M. Burša, L. Zach, M. Huptych, L. Lhotská, P. Janků, and L. Hruban, "Stability of variability features computed from fetal heart rate with artificially infused missing data," in *Computing in Cardiology (CinC), 2012*. IEEE, 2012, pp. 917–920.

[12] V. P. Oikonomou, J. Spilka, C. D. Stylios, and L. Lhotská, "An adaptive method for the recovery of missing samples from fhr time series." in *CBMS*, 2013, pp. 337–342.

[13] C. E. Rasmussen, *Gaussian Processes for Machine Learning*. Citeseer, 2006.

[14] V. Chudáček, J. Spilka, M. Burša, P. Janků, L. Hruban, M. Huptych, and L. Lhotská, "Open access intrapartum ctg database," *BMC pregnancy and childbirth*, vol. 14, no. 1, p. 16, 2014.

[15] E. W. Abdulhay, R. J. Oweis, A. M. Alhaddad, F. N. Sublaban, M. A. Radwan, and H. M. Almasaeed, "Review article: non-invasive fetal heart rate monitoring techniques," *Biomedical Science and Engineering*, vol. 2, no. 3, pp. 53–67, 2014.

ISBN 978-0-9928626-7-1 © EURASIP 2017